Desalination and Water Treatment
www.deswater.com

doi: 10.5004/dwt.2023.29706

300 (2023) 36–43
July

Wastewater remediation using activated carbon derived from Alhagi plant

Alaa K. Mohammed*, Hadeel Faroak Hameed, Israa M. Rashid

Biochemical Engineering Department, Al-Khwarizmi College of Engineering, University of Baghdad, Baghdad 47024, Iraq, email: dr.alaa@kecbu.uobaghdad.edu.iq (A.K. Mohammed)

Received 18 February 2023; Accepted 17 June 2023

ABSTRACT

This work focuses on the use of biologically produced activated carbon for improving the physico-chemical properties of water samples obtained from the Tigris River. An eco-friendly and low-cost activated carbon was prepared from the Alhagi plant using potassium hydroxide (KOH) as an impregnation agent. The prepared activated carbon was characterised using Fourier-transform infrared spectroscopy to determine the functional groups that exist on the raw material (Alhagi plant) and Alhagi activated carbon (AAC). Scanning electron microscope–energy-dispersive X-ray spectroscope was also used to investigate the surface shape and the elements that compose the powder. Brunauer–Emmett–Teller surface area analysis was used to evaluate the specific surface area and pore size of the prepared AAC. This study investigated three influential variables: activation temperature, activation time and impregnation ratio (IR) (KOH: dried solid wt./wt.). Central composite design was used to determine the interactions between the influential variables. Results show that an activation temperature of 650°C, activation time of 2.5 h and IR of 1:2.6 are optimal for activated carbon preparation.

Keywords: Chemical activation; Potassium hydroxide; Activated carbon; Central composite design; Wastewater

1. Introduction

Freshwater is considered a renewable natural resource when carefully and wisely used. The freshwater available on earth is 2.5%, out of which 0.01% is available as surface water in the form of lakes, rivers ponds and swamps. Utilising our water resources wisely through reuse and recycling becomes very essential. Wastewater treatment is an important criterion to revive the water bodies [1–4].

Active carbon plays a vital role in the treatment of wastewater due to its adsorption capacity and antibacterial property [5,6]. Research on the production of active carbon has played a pivotal role and enables invention of environmentally stable and cost-effective treatment technologies for treating water/wastewater to satisfy the ever-increasing water quality standards [5,7–9].

Activated carbon is a porous carbonaceous material with substantial surface functional groups that are commonly applied for catalyst support, gas separation, adsorption, decolorising and electrodes [10]. Activated carbons with a high level of porosity have been produced from various amorphous carbon-based materials [5,11]. Depending on the raw material, they are mostly composed of carbon atoms that are arbitrarily substituted with other heteroatoms, such as oxygen, to form cross-linked aromatic sheets in an irregular pattern [12]. Commercially available activated carbons are still considered expensive given the use of non-renewable and rather costly resources, such as coal. This condition has sparked a surge in research toward the production of activated carbons using renewable and low-cost precursors [13,14].

Physical and chemical activation are the most common techniques for preparing activated carbons. Physical activation consists of carbonising the precursor at 400°C–500°C in an inert atmosphere, such as steam, CO_2 or N_2, to activate the resulting char. In the second step of the physical

* Corresponding author.

activation, the char is oxidized between 700 and 1,100°C in the presence of N_2, steam and CO_2. Chemical activation consists of mixing the precursor with several active agents, such as KOH, H_3PO_4, NaOH and $ZnCl_2$, thereby enabling the materials to form porous structures. The chemical activation technique uses lower time and temperatures than the physical activation technique. The activating chemicals operate as dehydrating agents, preventing the production of volatile substances or tars throughout the process; as a result, the yield of carbon is increased whilst the time and activation temperature are decreased [11,15].

Alhagi plant is a suitable material for use as a precursor in the activated carbon production. A Fabaceae plant genus is found in many Asian, Australian and European countries. Alhagi, also known as camel thorn, is a genus of plants with a wide range of uses, including feed and traditional medicine [16,17]. It is a good source of biomass because it can grow in a wide range of climatic conditions with little water, fertiliser or pesticide usage. It is also a cellulose-rich plant [18,19].

The most important parameters determining pore volumes of the prepared Alhagi activated carbon (AAC) and specific surface area are the impregnation ratio (IR), the activation time and the activation temperature. Specific surface areas and pore volumes of AAC are also influenced by other factors, such as carbonisation conditions, nitrogen flow rate, heating conditions and even the activation agent form [20,21].

Clean water for various uses can be produced by treating industrial and municipal wastewater to remove contaminants and make it potable. Activated carbon is typically used in this process following steps, such as flocculation and sedimentation. KOH was used as the activating agent during the chemical activation process to prepare AAC. Other important variables that influenced the process included the IR, activation temperature and activation time. AAC can be applied to wastewater treatment due to its low cost, high carbonaceous content and abundance of these wastes.

2. Materials and methods

2.1. Samples preparation of Alhagi plant

Alhagi plant was collected from some areas in Baghdad. The plant was washed well with distilled water several times to remove any contaminants collected with it. Then, the plant was dried at 60°C for 24 h and crushed to the required size of approximately 2 mm. The sample was dried and placed in a container for further processing.

2.2. Carbonisation and activation

The dried mass of Alhagi pieces prepared in the previous step was impregnated with KOH solution and left overnight to allow the chemical reagent (KOH) to be absorbed by the raw components. Different IRs were used (IR is the weight ratio of KOH: dried raw material). Then, the impregnated material was carbonised in a steel box in a furnace at various activation temperatures and times. Nitrogen gas was used as an inert gas during the carbonisation process to activate the carbonised material and assist pore formation in the material. The activated carbon was left for a few hours to cool to room temperature with the remaining nitrogen gas flow. Finally, the product was washed with distilled water to remove any residual KOH and dried overnight in an oven at 100°C. The product was placed in a desiccator to prevent contact with humidity.

2.3. Sample characterisation

Characterisation of the product was carried out to assign the best values of the operating conditions used for preparing activated carbon from the Alhagi plant using KOH solution as the activating agent.

2.3.1. Scanning electron microscope

Scanning electron microscope (SEM) was used to investigate the surface shape and its topographical properties. The obtained images are 3D and represent the surface shape accurately. The elements of the precursors were analysed with an energy-dispersive X-ray spectroscope (EDS). SEM-EDS analysis was carried out by TESCAN VEGA III Electron Microscope (Czech Republic).

2.3.2. Fourier-transform infrared spectroscopy

Fourier-transform infrared spectroscopy (FTIR, IRAffinity-1, Shimadzu, Japan) was used to determine the functional groups in the Alhagi plant and AAC.

2.3.3. Brunauer–Emmett–Teller

Brunauer–Emmett–Teller (BET, HORIBA, SA-900 Series, USA) was used to determine the specific surface area of the prepared activated carbon. The pore-size distribution and BET surface area were determined by adsorption and desorption data of liquid nitrogen.

2.4. Sample preparation of water

The water samples were collected from the Tigris River, which is the second largest river in Western Asia. Many factories and industrial facilities on the banks of the river dispose their wastewater. These samples were collected in sterile plastic cans washed with 2% of HCl. The water was subjected to physico-chemical parameters using standard methods [15,22].

2.5. Wastewater treatment

A known weight of active carbon as adsorbent (0.3, 0.5 and 1 g) was added to 100 mL of water sample into different flasks.

The solution in each flask was stirred continuously in a shaker at 250 rpm at a room temperature of 25°C ± 2°C for 8 h. The solution was then filtered using Whatman No. 1 filter paper.

2.6. Experiment design

Central composite design (CCD) software is a commonly used statistical approach for optimising the

processing parameters and determining the regression model equations from the experimental results. It can also be used to investigate the interactions between the various parameters influencing the process response [23].

A significance level (α) of 0.05 is always selected for the experimental design. If the p-value is less than 0.05, then the parameter statistically exhibits a significant effect on the response; otherwise, no statistically significant association exists between the variables and the response [24].

The significance of the model equation can be determined using the F-test by comparing the F-test value to the tabulated F-values. The mathematical model is well-fitted to the experimental data if the calculated F-value is higher than the tabulated F-value. In addition, the high F-value of the studied parameters indicates significance [25].

The polynomial equation linking the response with the independent variables is suggested by the software in Eq. (1), as follows:

$$f(x) = a_0 + \sum_{i=1}^{N} b_i x_i + \sum_{i=1}^{N} c_{ii} x_i^2 + \sum_{ij(i<j)}^{N} c_{ij} x_i x_j + \sum_{i=1}^{N} d_i x_i^3 + \sum_{i=1}^{N} e_i x_i^4 \quad (1)$$

One of the research objectives is to produce activated carbon from Alhagi and find the optimum production conditions. Generally, many factors affect the AAC production by chemical activation, such as activation time, activation temperature and IR. CCD was used to investigate the effects of these factors. The ranges of the selected effective variables were as follows: activation temperature (500°C–800°C), impregnation ratio IR (1:1–1:3) and activation time (1–4 h). The response is the specific surface area (SSA) of the prepared activated carbon.

3. Results and discussion

3.1. Characterisation of the activated carbon

3.1.1. Scanning electron microscope

SEM was carried out to observe the morphology of the precursor surface, Alhagi powder (ALH) and the prepared AAC. Fig. 1a shows the surface nature of the ALH, which has low porosity, whereas Fig. 1b shows that the surface nature of AAC is porous and loose. Activation results indicate a large number of pores, are full of cavities, and are quite irregular. The reaction between carbon atoms and KOH, as well as the impact of high temperature on the activation process, results in different pore shapes, as shown in Fig. 1.

Elemental compositions of raw material (Alhagi) and AAC were investigated by EDS, and the results are shown in Figs. 2 and 3, respectively. The figures clearly show that the carbon percentage for active carbon produced from raw Alhagi plant is raised from 57.38% to 97.76%. Whereas all element compositions are reduced due to the carbonisation process or evaporation. The presence of potassium (K) may be due to the decomposition of residual traces of potassium hydroxide (KOH).

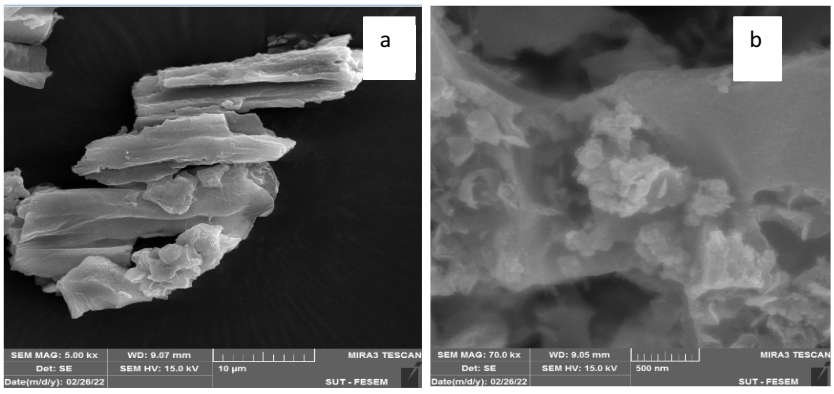

Fig. 1. Scanning electron microscope images of (a) Alhagi powder and (b) Alhagi activated carbon.

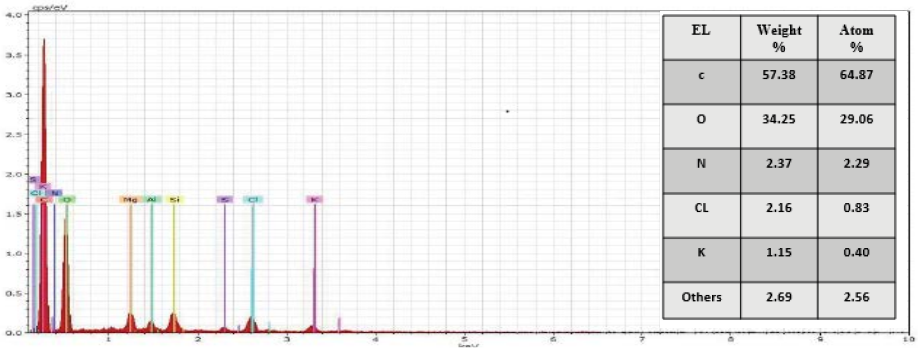

EL	Weight %	Atom %
c	57.38	64.87
O	34.25	29.06
N	2.37	2.29
CL	2.16	0.83
K	1.15	0.40
Others	2.69	2.56

Fig. 2. Energy-dispersive X-ray spectroscope analysis of Alhagi plant.

3.1.2. FTIR analysis of ALH and AAC

Fig. 4 shows the FTIR spectra for ALH and AAC. The broad peak that appears at approximately 3,298.28 cm^{-1} in ALH is assigned to the hydroxyl group. This finding indicates the presence of moisture that disappears from AAC spectra due to its elimination by the activation process. The band at 2,916.37 cm^{-1} in ALH is ascribed to alkane (C–H) stretching vibration, and the fading of this peak from ALH spectra indicates hydrogen removal during the activation process. The bands at 1,612.49 and 1,411.89 cm^{-1} in the ALH and AAC spectra, respectively, are due to the skeletal C=C vibrations of organics. The peaks of 667.37 and 709.80 cm^{-1} in the spectra of ALH and AAC, respectively, are assigned to the bending vibration of carbon bonds (C≡C). The band at 1,099.43 cm^{-1} in ALH has been assigned to (–C–O–C–) stretching. The bands at 1,141.86 cm^{-1} in AAC have been assigned to (C–O) stretching, and the bands at 1,018.41 and 871.82 cm^{-1} have been assigned to (C–H plane) and (C–H bend) stretching, respectively [26].

3.1.3. Surface area and pore structure

BET technique was used to determine the specific surface area of the prepared activated carbon. The BET analysis showed that the specific surface area was 738 m^2/g, and the average pore diameter was 4.1 nm.

3.2. Surface area of the activated carbons

The values of the effective parameters and the results of the activated carbon are shown in Table 1. The values of the parameters were selected according to the CCD program, whereas the yield and specific surface area (SSA) were experimentally evaluated. The increase in activation temperatures from 500°C to 800°C more effectively improves the SSA. The finding demonstrates that the structure has the propensity to become microporous as the activation temperature rises because KOH evaporation, which creates porosity, causes more KOH to evaporate as temperature increases, thereby enhancing the microporosity. On the contrary, SSA declined at 800°C, probably due to pore expansion brought about by high activation temperatures, which decreased the specific surface area values [9]. The sample with an IR value of 1:3 (Run No. 6), activation time of 2.5 h and activation temperature of 650°C shows a maximum yield of 46.14%, whereas the sample with an IR of 1:2.6 (Run No. 16), activation time of 2.5 h and activation temperature of 725°C shows a maximum SSA of 738 m^2/g.

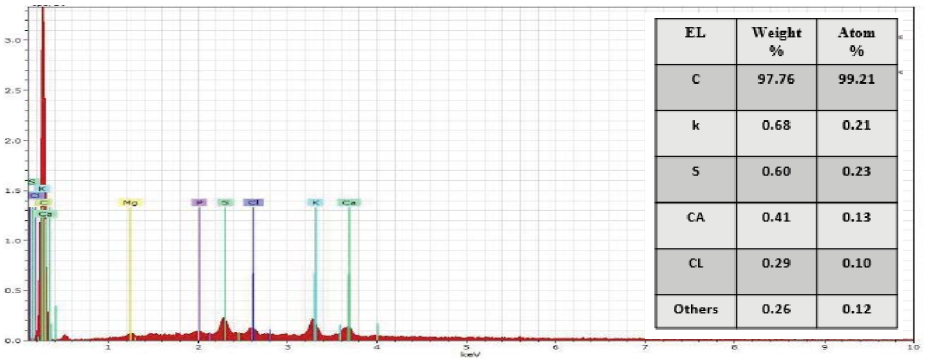

Fig. 3. Energy-dispersive X-ray spectroscope analysis of Alhagi activated carbon.

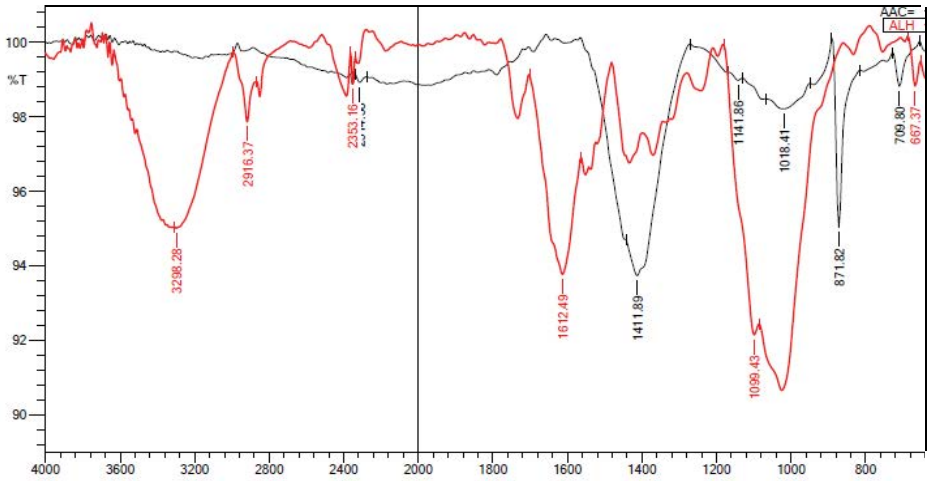

Fig. 4. Fourier-transform infrared spectra of Alhagi plant (ALH) and Alhagi activated carbon.

3.2.1. Interactive effect of IR and activation time

The effect of IR and time interaction is demonstrated in Fig. 5. The curves show that the SSA of activated carbon tends to increase as the IR rises until it reaches a value of approximately 1:2.6. Pore formation is influenced by the impregnation ratio. The intercalation of potassium metal into the carbon structure promotes pore formation. Thus, high impregnation ratio increases the amount of potassium metal that can be intercalated and promotes more pore formations. This condition results in an increase in the surface area and yield. Moreover, the effect of the time parameter is evident. The contour curves show that with the increase in activation time, the SSA increases gradually at the beginning and reaches optimum at an activation time of 2.6 h. The SSA increases with activation time because more carbon atoms at the active sites react with the activation agent and form a new pore structure, and the activating reaction reaches a full stage. Then, the curve begins to form into a stable shape because carbon atoms on the carbon skeleton are consumed and original micropores develop into micropores, resulting in a decrease in SSA. This finding is consistent with the finding of [16] that examined the influence of the same experimental parameters on the SSA of activated carbon produced from Alhagi. Therefore, the optimised values of IR and activation time obtained using CCD software are 1:2.6 and 2.6 h, respectively.

Table 1
Predicted values of yield and surface area using central composite design software

Runs	IR: *A*	Time: *B* (h)	Temp: *C* (°C)	Yield: R	Surface area: SA (m^2/g)
1	1:2	2.5	650	40%	500
2	1:2.6	1.75	725	40.24%	730
3	1:2.6	1.75	575	39%	460
4	1:2	1	650	28.04%	514
5	1:1.5	3.25	725	14.66%	715
6	1:3	2.5	650	46.14%	675
7	1:2	4	650	34.36%	630
8	1:2.6	3.25	575	45%	462
9	1:1.5	1.75	725	22.3%	689
10	1:1.5	3.25	575	35.56%	482
11	1:1.5	1.75	575	24.44%	472
12	1:2	2.5	650	42.42%	490
13	1:2	2.5	500	31%	452
14	1:2	2.5	800	18.6%	722
15	1:1	3.25	650	12.46%	488
16	1:2.6	2.5	725	33.63%	738

3.2.2. Interactive effect of the IR and activation temperature

The interactive effect of the IR and activation temperature is shown in Fig. 6. The contour plot indicates that the optimum value of temperature is 640°C and the IR is 1:2.6. The SSA of AAC increased until it reached an optimum value at nearly 640°C as the activation temperature increased from 500°C to 800°C. These results indicate that as the activation temperature increased, the structure tended to become more porous due to KOH evaporation. Subsequently, the SSA starts to decrease because high activation temperatures caused pore explosion, resulting in reduced SSA values [7].

3.3. Analysis of variance

Statistical significance of the factors was established with analysis of variance. IR was encoded as (*A*), time of activation (*B*) and temperature (*C*); SSA was also considered. The experimental values obtained from the lab experiments were compared with the predicted results calculated by statistical design software. R^2 is 0.9696, indicating that the

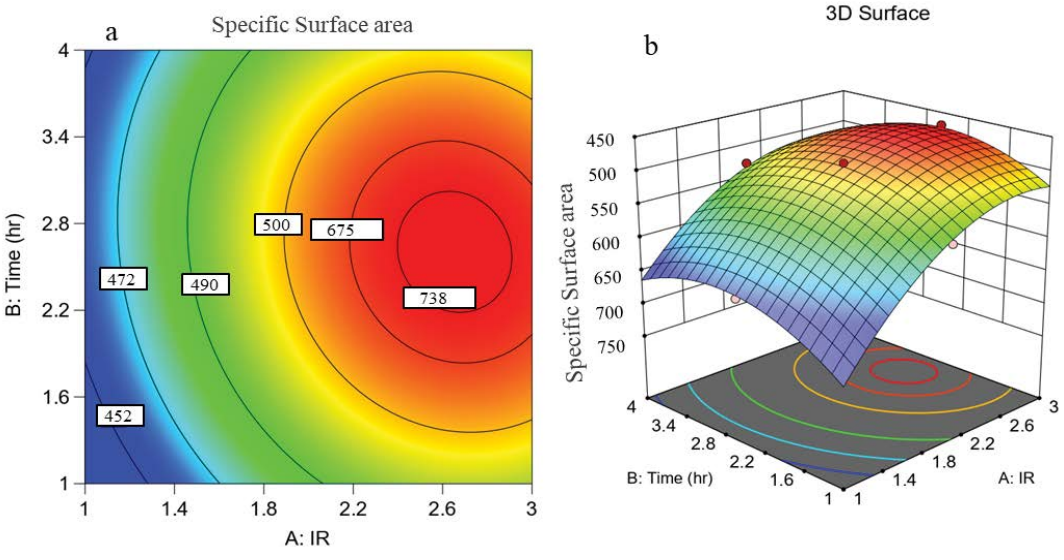

Fig. 5. Interaction between the impregnation ratio and time (a) contour and (b) 3D surface.

experimental data fit perfectly with the quadratic model. Fig. 7 plots the predicted values vs. experimental values of the SSA, which is a good tool in studying the significance of the suggested model. The plot shows that all the data points are close to the line, indicating that the experimentally observed data fit well with the empirical model.

The model equation for SSA is shown mathematically in Eq. (2) in terms of coded factors. The terms express the relationship between the independent variables and the dependent response of the system.

$$\begin{aligned}\text{SSA} = {} & 81.32 + 8.02A + 0.97B - 3.62C \\ & - 0.5100AB + 1.61AC - 3.92BC \\ & - 2.98A^2 - 2.50B^2 - 4.10C^2 \end{aligned} \quad (2)$$

Table 2 shows that according to the lower *p*-value and higher *F*-value, the most significant parameter is the IR,

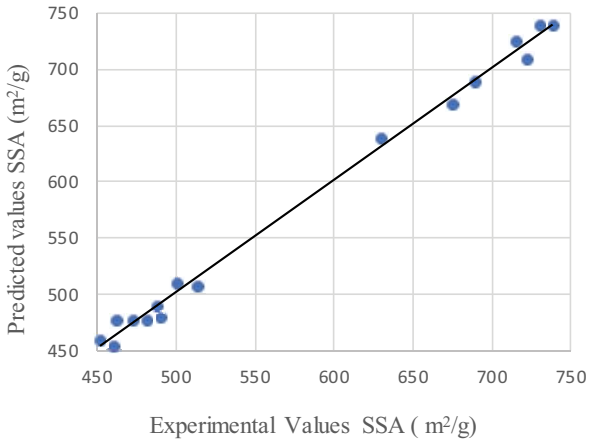

Fig. 7. Predicted vs. experimental values of the specific surface area of the prepared activated carbon.

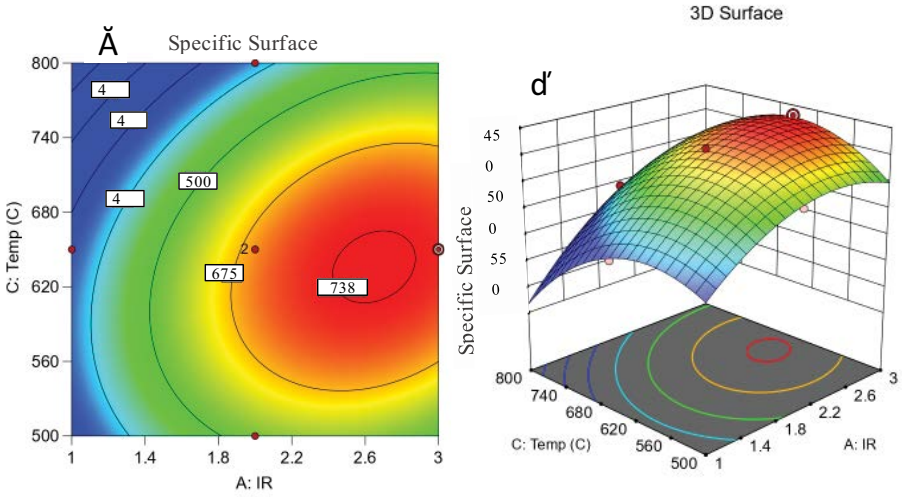

Fig. 6. Interaction between the impregnation ratio and temperature (a) contour and (b) 3D surface.

Table 2
Analysis of variance for quadratic model

Source	Sum of squares	df	Mean square	*F*-value	*p*-value	
Model	1,687.46	9	187.50	54.11	<0.0001	Significant
A-IR	1,028.48	1	1,028.48	296.79	<0.0001	
B-time	15.05	1	15.05	4.34	0.0822	
C-temp	209.96	1	209.96	60.59	0.0002	
AB	2.08	1	2.08	0.6005	0.4678	
AC	20.87	1	20.87	6.02	0.0495	
BC	122.93	1	122.93	35.47	0.0010	
A^2	141.85	1	141.85	40.93	0.0007	
B^2	100.20	1	100.20	28.91	0.0017	
C^2	269.29	1	269.29	77.71	0.0001	
Residual	20.79	6	3.47			
Lack of fit	17.86	5	3.57	1.22	0.5932	Not significant
Pure error	2.93	1	2.93			
Cor. total	1,708.25	15				

and the activation temperature has weak effect on time. Moreover, the more effective interaction is between the temperature and time.

3.4. Physico-chemical parameters

The effect of adsorbent dose in removing pollutants was investigated using various adsorbent doses. Experiments were carried out with the initial pollutant concentration presented in Table 3 (pretreatment results of wastewater). The physico-chemical analysis carried out for treated water sample is also presented in Table 3.

Fig. 8 shows the effect of adsorbent dosage on the sorption capacity of the solution. This figure indicates the efficiency of pollution removal as a function of various amounts of AAC. Evidently, increasing the sorbent dosage from 0.3 to 1 g/100 mL increases efficiencies. This finding was expected because the higher concentration of sorbents in the solution indicates larger availability of sorption sites. Therefore, when more AAC particles are available, more surface-active sites for pollutant molecules can be contacted, thereby accelerating the removal efficiency [28].

4. Conclusion

The present study aims to prepare activated carbon with a record high unit surface area from the Alhagi plant by chemical activation with KOH. Three parameters that affect the production of AAC by chemical activation, such as activation time, activation temperature and IR, were examined. The SSA of the produced activated carbon was selected as a response. The effects of the experimental parameters were investigated using CCD software. The optimum values of variables for AAC were IR of 1:2.6 at 725°C and activation

Table 3
Physico-chemical analysis for wastewater before and after treatment with Alhagi activated carbon

Physical properties	WHO standards [27]	Pretreatment results of wastewater	Post treatment results of wastewater			Removal%		
			30 g/L	50 g/L	100 g/L	30 g/L	50 g/L	100 g/L
pH	6.5–8.5	6.5	6.5	6.5	6.5	–	–	–
Electrical conductivity	1,000	1,322	1,222	1,153	1,100	7.7%	12.8%	16.8%
Total dissolved solids (mg/L)	500	520	500	480	460	3.85%	7.7%	11.5%
Total suspended solids (mg/L)	25	496	200	98	20	59.7%	80.2%	96%
Biological oxygen demand (mg/L)	<5	154	93	36	1.9	39.6%	76.6%	98.8%
Chemical oxygen demand (mg/L)	20–200	400	301	165	62	24.8%	58.8%	84.5%
Salinity (S‰)	<5	0.5	0.43	0.3	0.12	14%	40%	76%
Transparency (Trans)	12–75.3	67	59	41	23	11.9%	38.8%	65.7%
Chemical properties								
Calcium (Ca^{+2}) (mg/L)	200	160	150	108	60	6.25%	32.5%	62.5%
Chloride ions (Cl^{-}) (mg/L)	250	200	195	135	55	2.5%	32.5%	72.5%
Magnesium (Mg^{+2}) (mg/L)	200	72	68	54	21	5.56%	25%	70.8%
Phosphate (PO_4) (mg/L)	5.5	1.4	1.253	0.84	0.423	10.5%	40%	97.7%
Sulfates (SO_4) (mg/L)	200	250	240	222	198	4%	11.2%	20.8%
Total hardness (mg_{CaCO3}/L)	<500	650	631	534	422	2.9%	17.85%	35.1%
Total organic carbon (%)	2.7–21.1	24	21	18	14	12.5%	25%	41.6%

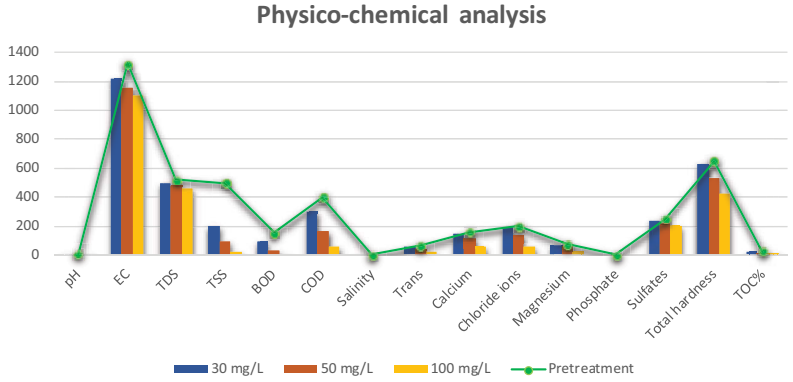

Fig. 8. Effect of adsorbent dosage on the sorption capacity of solution.

time of 2.5 h, providing the highest SSA of 738 m^2/g. R^2 is 0.9696, indicating that the experimental data fit perfectly with the quadratic model. The final product was characterised by SEM, FTIR and BET analysis. The results show that the carbon percentage of the activated carbon produced from raw Alhagi plants increased from 57.38% to 97.76%, whereas all element compositions decreased. The SSA of the prepared activated carbon was 738 m^2/g, and the average pore diameter was 4.1 nm.

Acknowledgements

We would especially want to thank and appreciate the biochemical engineering department of AL Khwarizmi Engineering College at University of Baghdad for assisting in the completion of this work.

Declaration of competing interest

The authors declare no conflict of interest in the submission of this paper. All authors agreed that this paper be published in 'Desalination and Water Treatment'.

Sources of financing format

No special funding was provided for this study by the government, businesses or nonprofit organisations.

Data availability

The data used are confidential.

References

[1] A.J. Adur, N. Nandini, Activated carbon impregnated with silver nanoparticles for remediation of wastewater, Int. Res. J. Commer. Arts Sci., 11 (2020) 52–57.
[2] M.M.H. Hammad, K.W. Hameed, H.A. Sabti, Reducing the pollutants from municipal wastewater by *Chlorella vulgaris* microalgae, Al-Khawarizmi Eng. J., 15 (2019) 97–108.
[3] M.I. Din, R. Khalid, Z. Hussain, I. Majeed, J. Najeeb, M. Arshad, Preparation of activated carbon from *Salvadora persica* for the removal of Cu(II) ions from aqueous media, Desal. Water Treat., 266 (2022) 131–142.
[4] A. Gundogdu, P. Bozbeyoglu, M. Imamoglu, C. Baltaci, C. Duran, V.N. Bulut, Characterization of the adsorption mechanism of cadmium(II) and methylene blue upon corncobs activated carbon, Anal. Lett., 56 (2022) 433–448.
[5] S.D. Salman, Adsorption of heavy metals from aqueous solution onto sawdust activated carbon, Al-Khawarizmi Eng. J., 15 (2019) 60–69.
[6] S.D. Salman, I.M. Rasheed, M.M. Ismaeel, Removal of diclofenac from aqueous solution on apricot seeds activated carbon synthesized by pyro carbonic acid microwave, Chem. Data Collect., 43 (2023) 100982, doi: 10.1016/j.cdc.2022.100982.
[7] M. Waleed Khalid, S.D. Salman, Adsorption of chromium ions on activated carbon produced from cow bones, Iraqi J. Chem. Pet. Eng., 20 (2019) 23–32.
[8] S. Usanmaz, Ç. Özer, M. İmamoğlu, Removal of Cu(II), Ni(II) and Co(II) ions from aqueous solutions by hazelnut husks carbon activated with phosphoric acid, Desal. Water Treat., 227 (2021) 300–308.
[9] Ç. Özer, M. İmamoğlu, Isolation of nickel(II) and lead(II) from aqueous solution by sulfuric acid prepared pumpkin peel biochar, Anal. Lett., 56 (2022) 491–503.
[10] R. Rohatgi, A.K. Kapoor, Development of latent fingerprints on wet non-porous surfaces with SPR based on basic fuchsin dye, Egypt. J. Forensic Sci., 6 (2016) 179–184.
[11] N.M. Jabbar, S.D. Salman, I.M. Rashid, Y.S. Mahdi, Removal of an anionic Eosin dye from aqueous solution using modified activated carbon prepared from date palm fronds, Chem. Data Collect., 42 (2022) 100965, doi: 10.1016/j.cdc.2022.100965.
[12] A.H. El-Sheikh, A.P. Newman, H.K. Al-Daffaee, S. Phull, N. Cresswell, Characterization of activated carbon prepared from a single cultivar of Jordanian Olive stones by chemical and physicochemical techniques, J. Anal. Appl. Pyrolysis, 71 (2004) 151–164.
[13] B.H. Hameed, J.M. Salman, A.L. Ahmad, Adsorption isotherm and kinetic modeling of 2,4-D pesticide on activated carbon derived from date stones, J. Hazard. Mater., 163 (2009)121–126.
[14] S.D. Salman, I.M. Rasheed, A.K. Mohammed, Adsorption of heavy metal ions using activated carbon derived from Eichhornia (water hyacinth), IOP Conf. Ser.: Earth Environ. Sci., 779 (2021) 012074, doi: 10.1088/1755-1315/779/1/012074.
[15] H. Zhang, Y. Yan, L. Yang, Preparation of activated carbons from sawdust by chemical activation, Adsorpt. Sci. Technol., 26 (2008) 533–543.
[16] G.M. Abd-Hadi, S.D. Salman, Adsorption of para nitro-phenol by activated carbon produced from Alhagi, Sains Malays., 49 (2020) 57–67.
[17] G. Muhammad, M.A. Hussain, F. Anwar, M. Ashraf, A.H. Gilani, Alhagi: A plant genus rich in bioactives for pharmaceuticals, Phytother. Res., 29 (2015) 1–13.
[18] Z. Nezafat, M. Nasrollahzadeh, Biosynthesis of Cu/Fe_3O_4 nanoparticles using *Alhagi camelorum* aqueous extract and their catalytic activity in the synthesis of 2-imino-3-aryl-2,3-dihydrobenzo[d]oxazol-5-ol derivatives, J. Mol. Struct., 1228 (2021) 129731, doi: 10.1016/j.molstruc.2020.129731.
[19] H.M. Abdul-Hameed, Adsorption of Cd(II) and Pb(II) ions from aqueous solution by activated carbon, Al-Khawarizmi Eng. J., 5 (2009) 13–17.
[20] A. Kumar, H.M. Jena, Preparation and characterization of high surface area activated carbon from Fox nut (*Euryale ferox*) shell by chemical activation with H_3PO_4, Results Phys., 6 (2016) 651–658.
[21] H.F. Hameed, A.K. Mohammed, D.S. Zageer, Comparative study between activated carbon and charcoal for the development of latent fingerprints on nonporous surfaces, Al-Khawarizmi Eng. J., 18 (2022) 1–13.
[22] S.M. Khalaf, F.M. Hassan, A.H.J. Al-Obaidy, Detection of polycyclic aromatic hydrocarbons compounds concentrations and their fate in Tigris River within Baghdad City - Iraq, Iraqi J. Agric. Sci., 50 (2019) 231–244.
[23] B. Sadhukhan, N.K. Mondal, S. Chattoraj, Optimisation using central composite design (CCD) and the desirability function for sorption of methylene blue from aqueous solution onto *Lemna major*, Karbala Int. J. Mod. Sci., 2 (2016) 145–155.
[24] A.E. Sarrai, S. Hanini, N.K. Merzouk, D. Tassalit, T. Szabó, K. Hernádi, L. Nagy, Using central composite experimental design to optimize the degradation of Tylosin from aqueous solution by photo-Fenton reaction, Materials (Basel), 9 (2016) 428, doi: 10.3390/ma9060428.
[25] S. Chattoraj, B. Sadhukhan, N.K. Mondal, Predictability by Box–Behnken model for carbaryl adsorption by soils of Indian origin, J. Environ. Sci. Health., Part B, 48 (2013) 626–636.
[26] T. Budinova, E. Ekinci, F. Yardim, A. Grimm, E. Bjornbom, V. Minkova, M. Goranova, Characterization and application of activated carbon produced by H_3PO_4 and water vapor activation, Fuel Process. Technol., 87 (2006) 899–905.
[27] M.K. Mensoor, Monitoring pollution of the Tigris River in Baghdad by studying physico-chemical characteristics, Res. Square, (2021) 1–17, doi: 10.21203/rs.3.rs-1074093/v1.
[28] A. Al-Fatlawi, M.M. Neamah, Batch experiment and adsorption isotherm of phosphate removal by using drinking water treatment sludge and red mud, Int. Adv. Res. J. Sci. Eng. Technol., 2 (2015) 557–571.